This is a repository copy of *Systems and synthetic biology of the vessel wall.*.

White Rose Research Online URL for this paper:
https://eprints.whiterose.ac.uk/178759/

Version: Published Version

Article:

FEBS Letters

Review

Systems and synthetic biology of the vessel wall

Jennifer Frueh, Nataly Maimari, Ying Lui, Zoltan Kis, Vikram Mehta, Negin Pormehr, Calum Grant, Emmanuel Chalkias, Mika Falck-Hansen, Sandra Bovens, Ryan Pedrigi, Taka Homma, Gianfillippo Coppola, Rob Krams *

Department of Bioengineering, Imperial College London, United Kingdom

A B S T R A C T

Atherosclerosis is intimately coupled to blood flow by the presence of predilection sites. The coupling is through mechanotransduction of endothelial cells and approximately 2000 gene are associated with this process. This paper describes a new platform to study and identify new signalling pathways in endothelial cells covering an atherosclerotic plaque. The identified networks are synthesized in primary cells to study their reaction to flow. This synthetic approach might lead to new insights and drug targets.
© 2012 Federation of European Biochemical Societies. Published by Elsevier B.V.

1. Introduction

Coronary heart disease (CHD) is the global leading cause of death. In the UK, acute coronary syndromes (ACS) cause ~60% of CHD deaths and lead to ~240,000 hospitalizations each year, incurring direct healthcare costs of ~£1.7 billion annually. The majority of the mortality of CHD is related to the rupture of a thin cap fibroatheroma (TCFA). The characteristics of a rupture-prone plaque are that of a large and soft lipid-rich necrotic core covered by a thin and inflamed fibrous cap [1,2]. Associated features include big plaque size, expansive remodelling preventing luminal obstruction (mild stenosis by angiography), neo-vascularization, plaque haemorrhage, adventitial inflammation, and a "spotty" pattern of calcifications [1,2]. While cross sectional composition of plaques is known and have been described extensively, the longitudinal heterogeneity of plaques has recently attracted more attention [3–5].

The rediscovery of longitudinal plaque heterogeneity exposed an essential role for blood flow determining plaque composition. Recent studies, including ours, showed that (local) shear stress is a better predictor of plaque composition than plaque size or (bulk) cholesterol levels [1,3,6–10]. To further investigate the role of shear stress in plaque composition, we *induced* two different pro-atherogenic shear stress fields (low, non-oscillatory and low, oscillatory shear stress patterns) in a straight vessel of hypercholesteremic, ApoE −/− mice and demonstrated that specific shear stress patterns *induced* specific plaque compositions, when ApoE −/− mice were exposed to a high cholesterol environment [11–13]. Interestingly, the low, non-oscillatory shear stress pattern induced TCFAs, while the low and oscillatory shear stress induced stable plaques [12–15]. Further studies indicated that TCFA formation was associated with the presence of adhesion factors, chemokines, and activating factors for macrophages [12–15], indicating that the reduction of blood velocity enhanced inflammation in the plaques. These observations have recently been confirmed in pig coronary arteries, and in human carotid and coronary vessels indicating that blood flow and its derivative, shear stress (which scales linearly to velocity) is fundamental to determining plaque composition [16–18].

All studies above indicate that the flow-directed phenotype of the endothelial cell determines the processes leading to TCFA formation. Endothelial cells are known to contain a variety of mechanosensors and two decades of research have identified that seven-nine endothelial pathways are modified by mechanical stimulation. These mechano-sensitive pathways regulate eight acknowledged transcription factors, which lead to the expression of ~2000 genes [7,19–24]. The sheer number of mechano-sensitive

pathways, their interactions, and their unknown dynamics in endothelial cells covering a plaque offers a challenging problem, to identify individual signalling cascades.

Several methods are emerging from the field of systems biology to solve these intractable problems, which may roughly be divided in two ways: bottom-up and top-down approaches. The bottom-up strategy characterises small signalling networks by applying a combination of genomics and systems biology, while exposing cells to an environment of atherogenic risk factors [25–27]. In the second (top-down) strategy one aims to use high throughput genomic screens and state-of-the art bioinformatics analysis methods to identify (small) gene networks of interest [28–31]. While both methods will lead to small networks amenable to a synthetic biology approach, the top-down method often needs an extra step of validation before the synthetic biology networks may be constructed.

In this article, we describe a new platform which aims to combine state-of-the-art 3-D imaging, computational modelling, cutting-edge genomics, bioinformatics and systems biology to decipher, old and new signalling pathways in endothelial cells which will be used to rationally design new synthetic networks aimed at treating atherosclerosis. In order to do so, we have developed a novel platform for cardiovascular studies (Fig. 1). The details of the platform will be discussed in larger detail below, and the first studies using (parts of) this platform are presented in this paper. Initiatives to study these networks using synthetic methods are also presented.

2. Material and methods

2.1. Systems and synthetic platform for vascular studies

In recent years, we have developed a comprehensive, modular imaging platform to combine state-of-the art imaging, computational methods with 3-D histological reconstruction techniques which enables us to couple high resolution geometry of the plaque to shear/wall stress and protein distribution (see Fig. 2), described before. Briefly, we combine microCT with microMRI to obtain two

Systems and synthetic platform for vascular studies

Preprocess
- Imaging: μCT, μMRI, μscope
- Segmentation, 3D-reconstruction
- Computational Fluid Dynamics (CFD)

Genomics
- Cell Isolation, RNA isolation, Laser Capture, Deconvolution
- Microarray analysis, Next Generation Rapid Sequencing

BioInf
- Co-expression analysis for Gene Networks
- Essential small networks

SynBio
- Synthetic Biology of small networks
- Testing new strategies
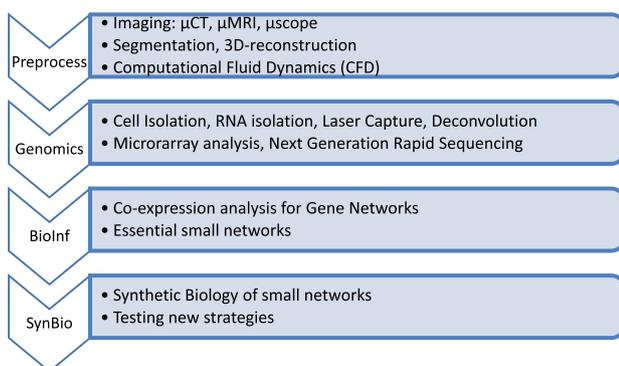
Fig. 1. This figure describes the platform used to identify small networks from situations where vascular disease can be mimicked realistically. To that end a modular image–based front has been designed that captures images, segments images and performs biomechanical calculations to isolate regions of interest. These regions are then used to isolate cells of interest with either laser capture techniques, or statistical deconvolution (see text for further details) in order to obtain cellular RNA from regions of interest. This RNA is then used for high throughput analysis with microarrays or RNA-seq, pre-processed and normalised. The resulting set of differentially expressed genes is analysed with state-of-the art bioinformatics software (time-dependent ARACNE) to obtain the topology of the networks. This topology matrix is then used to solve a linear system model which captures the flux dynamics of the network of interest.

contours from the lumen-vessel wall interface and from the vessel wall-adventitia interface. These contours are used to warp the cross sections, shrunken by their histology treatment, back into their original geometry, allowing individual cross sections to be reconstructed in 3-D dimensions (Fig. 2). The coupling to 3-D histological methods – as presented here – preserves the high spatial resolution needed to accurately map the large heterogeneity of atherosclerotic plaques in small animals. A further advantage of the current method is the usage of immunohistochemistry for protein detection, and the possibility to relate our biomechanical parameters to a wide variety of protein distributions. The high resolution 3-D lumen-vessel wall reconstruction is used for computational fluid dynamics. Features of the resulting stress/strain and/or protein distributions are used to identify regions of interest on digitally-derived cross sections (Fig. 3). These regions of interest steer a robot-driven laser-capture machine-microscope system (Zeiss, Munchen, Germany) which enables to identify and isolate cells of interest on basis of protein distribution and/or biomechanical profile. A non-contact technique is then used to isolate RNA from the selected cells (Fig. 3).

In conditions where cellular content is too low and RNA yield minimal, we use a statistical deconvolution technique for further analysis. This is a statistical approach of deconvolving gene expression profiles obtained from heterogeneous tissue samples into cell-type-specific sub-profiles. This method is based on a framework first proposed by Venet et al. [32], incorporating the assumption that the gene expression in a mixture of cell types is a weighted sum of those cell types. The weights are proportional to the relative contribution of these cell types in the mixture and are hence invariable among genes. Subsequent studies have demonstrated that the linearity assumption is valid under a wide variety of experimental conditions, especially when the cellular composition of the heterogeneous tissue was determined in the same object as where the RNA was obtained from [33,34]. To deconvolve cell-specific gene expression, we applied a statistical methodology of csSAM which, given microarray data from two groups of biological samples and the relative cell-type frequencies of each sample, estimates the average gene expression for each cell-type at a group level, and uses these cellular gene expression levels to identify differentially expressed genes at a cell-type specific level between experimental conditions.

These gene sets are subsequently analysed by Gaussian Graphical Modelling (GGM) to obtain the topology of biological networks of interest. GGM uses partial correlation to identify direct from indirect interactions between genes [35]. On selected networks, a stringent Gene Enrichment Analysis (GSEA) is used to identify groups of genes that act as a group within the network. When time dependent data are present, analysis based upon the time-delay ARACNE module is performed [36]. Finally, we are currently expanding these possibilities with ODEs, using (constrained) flux balance analysis [37–40] (Fig. 4).

2.2. Platform benchmarking

In order to test this platform, we have been studying tissue obtained from 240 ApoE −/− mice on a high cholesterol diet. Each animal was instrumented with a shear stress modifier, which has been shown to induce vulnerable and stable plaques in a single vascular segment [13,41]. The progression of plaque development has been fully characterised in previous studies and on basis of these studies, vascular tissue was isolated at 6 and 9 weeks of plaque development to study gene expression profiles from vulnerable and stable plaque regions [13,41]. On the basis of measured shear stress profiles [42], low shear stress induced vulnerable plaque and oscillatory shear stress stable plaque regions were selected on basis of which RNA was purified using the RNeasy

Preprocess module
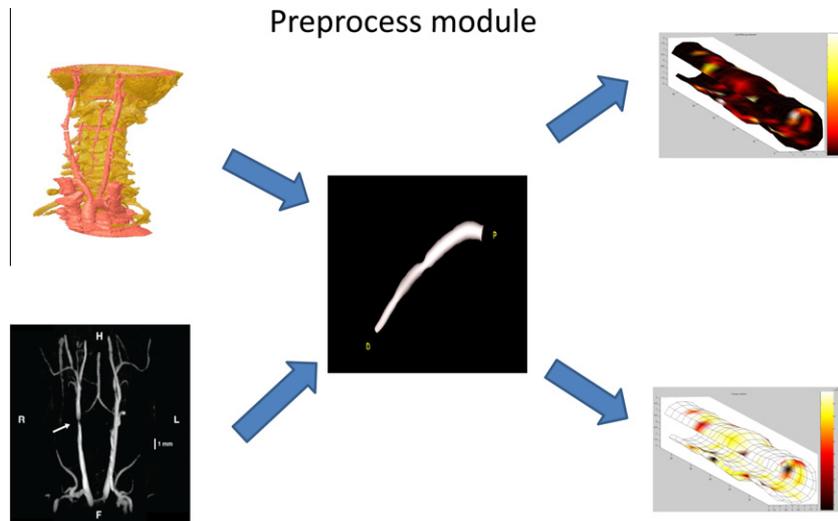
Fig. 2. Different imaging input modules are used to obtain an accurate geometry of the (diseased) vessels. A preference for high spatial resolution techniques (microscopy, micro-CT) is favoured over other techniques, albeit micro-MRI and ultrasound are often used to obtain functional information. State-of-the art segmentation techniques ('level-set methods') are used to identify the vessel wall, which is subsequently used to mesh either the vessel lumen or the vessel wall applying linear mapping techniques. to use computational techniques to obtain shear stress maps, or wall stress maps. High spatial resolution information from the vessel wall is obtained from an in-house developed 3-D imaging technique. An example on the right side of the pictures shows the 3-D distribution of lipids in a plaque, coupled to a 3-D young modulus distribution and a resulting mechanical stress distribution.

Genomics module
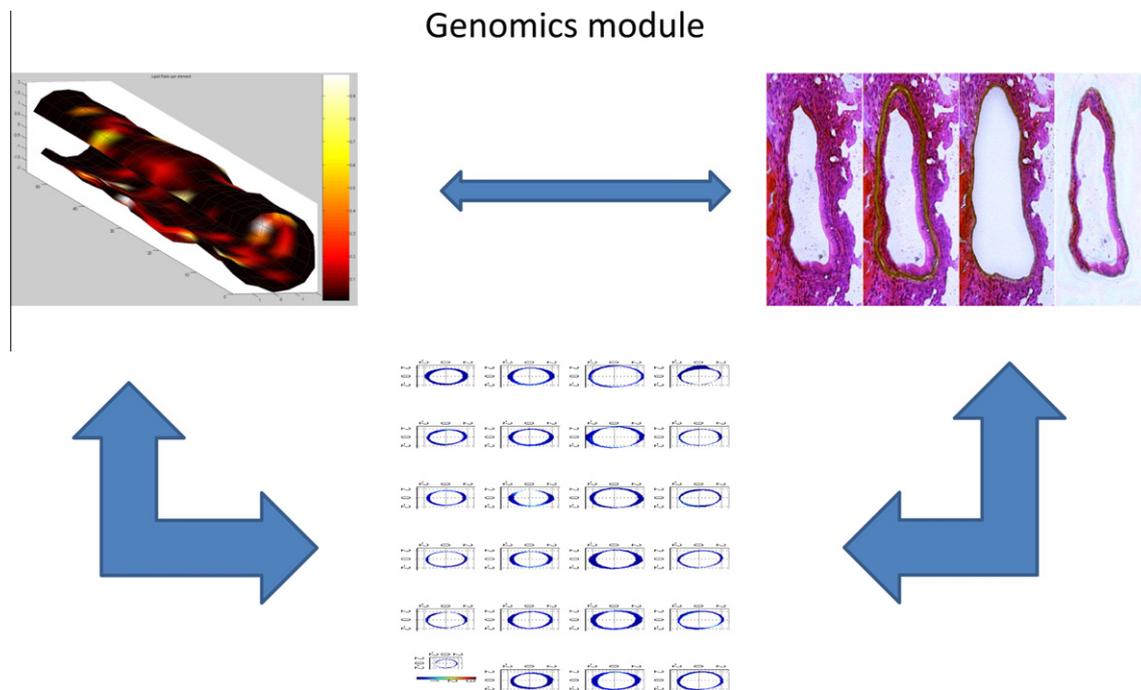
Fig. 3. From the 3-D colour distribution, regions in the vessel wall are isolated on features considered important for the process of interest. Colour coding may be related either to wall or shear stress distributions obtained from computational techniques or to any protein distribution derived by immunohistochemistry. The software then generates digital cross sections that serve as input for a robot-driven laser-capture machine. This machine automatically dissects the cells from the regions of interest and processes them to obtain cellular RNA. As sometimes the yield of RNA is too low, we have also developed a technique based upon statistical deconvolution, which allows obtaining cellular gene expression profiles from entire vessel wall, pooled RNA.

Micro kit with DNase treatment (Qiagen, Germany) according to manufacturer's protocol. After amplification and labelling of purified RNA samples, cDNA samples were hybridized to GeneChip Mouse Genome 430 2.0 arrays for 18 h (Affymetrix). Post-hybridization washing, scanning and image analysis were performed according to Affymetrix protocols. The yield of RNA at 6 and 9 weeks from these regions was of high quality, but too low for a single microarray experiment and 10 animals were subsequently pooled for a single microarray at each time point. A total of 6 microarrays for vulnerable and stable plaques were studied at 6 and 9 weeks of cuff placement (total of 24 arrays, obtained from 240 animals: Fig. 5).

Normalisation of the microarrays was based on quartile normalisation and gene-level signal estimates were generated using the Robust Multichip Average (RMA) algorithm implemented in Expression Console software provided by Affymetrix, including
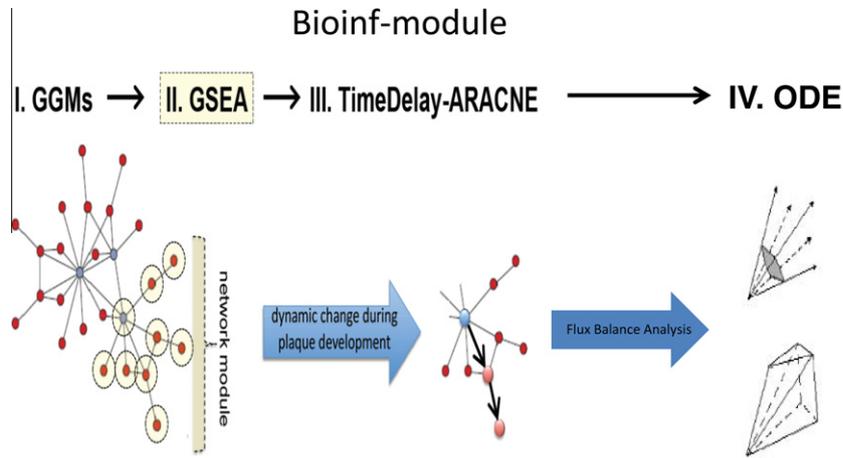
Fig. 4. This picture describes the bioinformatics platform developed by us, where we use a combination of GGM and GSEA to identify modules of networks, followed by ARACNE, when temporal data are present. While this approach offers the topology for a network, it does not necessary describes dynamics. This is acquired by implementing linear systems theory based flux based analysis, as a last and final step.
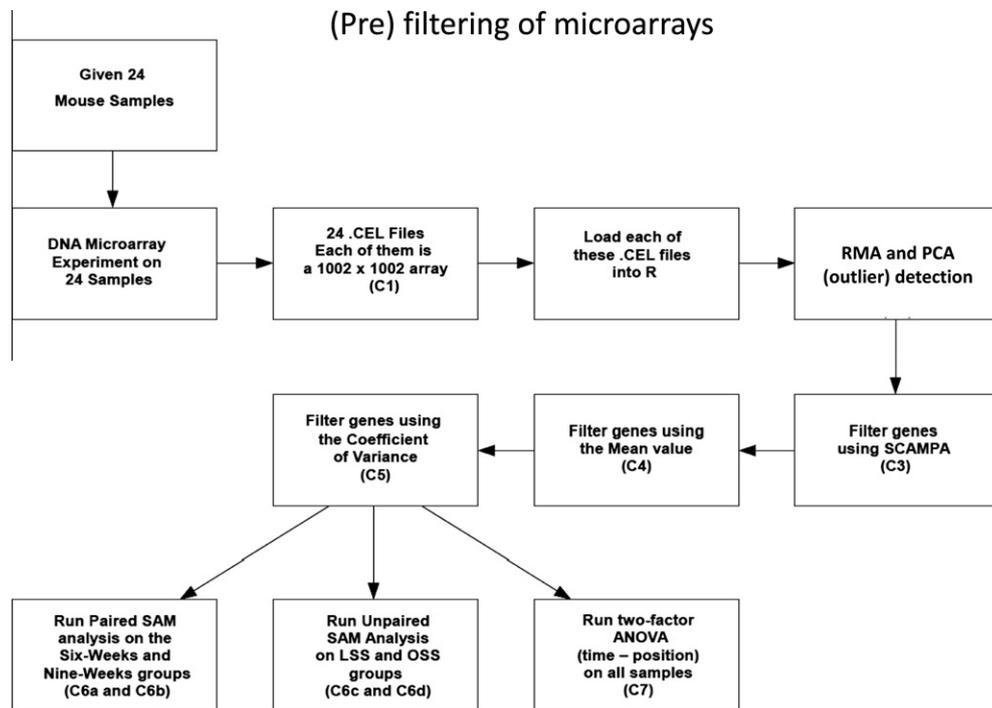
Fig. 5. This picture describes the filters used to describe the analysis of the microarrays. After normalising the microarrays with RMA, we performed a principal component analysis to identify homogeneity of sets of microarrays. Four arrays were found different than the clusters identifying each experimental condition and were deleted. The remaining 20 arrays were filtered using SCAMPA, for low expression using their mean value and for absence of change during experimental intervention using their variance. The remaining probe set was analysed in several ways using SAM, RANKPROD and ANOVA.

only core probe sets. RMA background corrects, normalises and summarises probe level intensities to provide low noise level gene expression values (Fig. 5). Next, Principal Component Analysis (PCA) was applied on the entire microarray to identify homogeneous sets. The analysis revealed that four of the microarrays LSS9W.3, OSS9W.4, LSS6W.4, LSS6W.6 deviated from the remainder of the set and could be identified as outliers, resulting in 20 microarray for further analysis (Fig. 5). Subsequently, several filters were developed to improve the signal to noise ratio of the remaining test. First SCAMPA was used to filter genes that were not annotated. Secondly, we filtered the genes whose mean value across all samples was lower than the 5% percentile, which signifies the probe sets with lowest expression levels and correspond to

background noise not directly relevant to our experiment. Thirdly, we filtered those genes whose Coefficient of Variation (CV) obtained over all samples was lower than the 5 percentile; that is, we deleted genes which showed smallest amount of change across all samples. After filtering, the final number of probe sets was reduced to 35,340 from 45,101 (Fig. 5).

3. Results

3.1. Whole-genome differential gene expression

We compared SAM and RANKPROD at a FDR level of 5% for whole genome differential gene expression levels. For LSS6W and

OSS6W SAM identified 9758 genes as significant while RankProd identified 3123genes and the combination of both identified 2815 genes; between groups of LSS9W and OSS9W: RankProd identified 513 significant genes and SAM did not detect any, so the overlap is 0; between groups of LSS6W and LSS9W: SAM identified 580 significant genes, RankProd identified 1152 genes and the overlap is 225 genes; between groups of OSS6W and OSS9W, 14285 genes were identified by SAM as significant, 3433 genes by RankProd and the overlap is 3226 genes.

3.2. Cell-specific differential gene expression

The Iterative Boolean procedure was tested against known cell fractions obtained from a separate series of experiments with a good result, indicating that the method to generate posterior PDFs of our cellular plaque compositions produced accurate results. Implementing the posterior PDF to the deconvolution method revealed new cell-specific genes that were undetected with the classical SAM method. A first analysis, where time and location were taken as independent variables, revealed that time was non-significant. Hence, the time-dependent samples were pooled to increase power of the tests. As a result, the number of genes differentially expressed between vulnerable and stable plaques were 16,645, distributed over VSMC (1300 genes), Endothelial Cells (6300), T-cells (4900), and Macrophages (5100).

3.3. Pathway selection

Pathway analysis was performed applying gene enrichment analysis – which identified 49 pathways, of which 4 were activated both in VSMC and ECs, and 45 pathways were exclusively activated in endothelial cells. Two pathways were selected for further study: the MAPK and PPAR pathways. The MAPK pathway is driving two very important mechanosensitive transcription factors: the NF-κB and KLF-2 pathways and, and consequently those TFs were further studied in larger detail.

3.4. The NF-κB and KLF2 pathways under flow

Based on the results presented above we decided to study the dynamic behaviour of the MAPK-NF-κB pathway and the MAPK5-KLF2 pathway in endothelial cells under well defined flow conditions in vitro. A step response in flow applied to an endothelial cell monolayer induced an oscillation of both pathways, depending on the level of blood flow. There was, however, a clear difference between both pathways, as the period of oscillation of the NF-κB pathway was 20 min, and that of the KLF-2 pathway was 2 h. For both pathways, there was an increase in frequency of oscillation when flow was increased. Frequency modulation has been identified as an emerging mechanism for gene regulation in a variety of cells under a diversity of experimental conditions [43–47], making it an important problem. At present its regulation is unknown and our group is studying this topic applying a combination of mathematical modelling and experimentation measurements.

The first systems model we designed was the MAPK/IKK/NF-κB pathway. This pathway is known to oscillate due to the presence of two negative feedback loops: one consisting of Iκ-B and NF-κB interaction and the second one of A20-IKK interaction [44,48]. Our initial model predictions indicated that the flow-dependent oscillations could not be caused by the accepted feedback loops (Iκ-B and A20), and we therefore gathered experimental evidence indicating that the regulation of the eNOS-NO pathway which is known to be controlled by NF-κB and its related nitric oxide release offers a new level of frequency modulated regulation. By parameter estimation techniques, taken into account NO transport and NO-inhibition studies by LNMA, we identified an unknown

influence of NO on IKK activity. Further analysis of the molecular structure of IKK identified 3 possible sites for nitrosylation. These sites are currently evaluated by site-directed mutagenesis.

We recently obtained evidence that, besides the oscillation of the NF-κB pathway, the MAPK5-MEF2c-KLF2 pathway also oscillates under flow. The reason for these oscillations is currently unknown and we have performed a microarray analysis to further elucidate the underlying mechanism. The initial results indicate the presence of a negative feedback loop at the level of MEF2c-KLF2 which might offer a new, initial explanation for this observation.

4. Discussion

This paper describes a new platform where sophisticated 3-D imaging and computational methods are used to identify cells of interest on basis of biomechanical features (shear stress and wall stress). The isolation of RNA from these cells, subsequent microarray analysis and statistical deconvolution methods identified a variety of signalling pathways unknown to endothelial cells covering a vulnerable plaque. One of these pathways, the MAPK pathway was selected for further studies, as it was one of the strongest activated signalling pathways in endothelial cells covering the vulnerable plaque and members of this pathway have been shown to react to blood flow in cultured cells. Two transcription factors regulated by the MAPK-pathway appeared to react to blood flow, and surprisingly oscillated with the level of blood flow. Mathematical systems models of these pathways identified new levels of regulation. These new findings were based upon two methods, which will be discussed in further detail.

Deconvolution of gene expression for heterogeneous samples can be performed accurately when sufficiently precise estimates of the proportional representation of component cell types in each sample is available and when expression profiles of the components are sufficiently different. Cell proportions can be measured through experimental methods such as fluorescence activated cell sorting analysis and histopathological evaluation. With known cell-type proportions in the mixture, deconvolution can be solved as a linear regression problem in which the cell-specific gene expression represents the regression coefficients [33,34].

When the proportions of the component cell types are unknown, there are investigations that performed deconvolution with expression of signature genes in pure cell types [49]. Abbas et al. [49] described a method to predict the proportions of white blood cell subtypes in samples from patients with systemic lupus erythematosus. First, they selected the most highly expressed signature genes from 18 immune cells according to their expression profiles for each cell population. Then they applied the expression data of these signature genes to solve a linear equation for the proportions of the 18 immune cell subtypes in both healthy donors and patients with lupus. [50] Using deconvolution, they quantified the constituents of real blood samples and mixtures of immune-derived cell lines and uncovered the correlations of leucocyte dynamics to clinical variables and measures. Under circumstances where careful preliminary studies have been conducted to identify expression profiles of signature genes from pure samples that clearly distinguish the cell types, such deconvolution can be successful.

Without the prior measurement of cell-type proportions or the identification of any signature genes, some studies used a variety of methods, such as Bayesian framework, non-negative matrix factorization and logarithmic data transformations [33,34,51–54].

Erkkilä et al. formalised a probabilistic model, DSection, and showed with simulations as well as with real microarray [55] data that DSection attains increased modelling accuracy in terms of estimating cell type proportions of heterogeneous tissue samples and identifying differential expression across cell types under various experimental conditions. They incorporated the missing

functionality of cell type proportions into the linear regression framework through Bayesian probabilities whose shapes reflect the uncertainties associated with the prior information, such as cell-type proportions or cell-type-specific expression profiles. For all model parameters, a Markov chain Monte Carlo (MCMC) sampler is proposed under the assumption that the heterogeneous tissues have been measured under various experimental conditions, which may have impact on cell-type-specific expression profiles [55].

We adapted this method to form a pipeline with the cell-type-specific significance analysis of microarray (csSAM) method developed by Shen-Orr et al. [56]. While these authors validated their method on synthetic mixtures of liver, brain and lung cells from rats and the mixture expression profiles obtained in silico turned out to be highly correlated with the experimentally measured expression profiles for the mixtures. The sub profiles of cell-specific expression deconvolved were in good agreement with expression measured in pure cell types for a large majority of probes. We concluded from these measurements that the combination of Markov-chain Monte Carlo modelling and csSAM seems to be a useful tool for analysis of gene expression from heterogeneous samples with unknown cell proportions. Indeed, our results show a good prediction of cell types, and a consistent gene expression at different levels of false discovery rates. Furthermore, the discovered signalling pathways were known to be shear dependent, which was confirmed under well-controlled flow conditions.

These small networks can now be tested with synthetic methods in a newly developed environment enabling to rapidly transfect primary cells with a large variety of small networks, while placed under complex biomechanical and chemical environments.

In conclusion, this paper describes a new platform that enables to identify new disease specific networks, applying a combination of imaging, computational modelling and state-of-the art genomics. The resulting small networks can be studied in cells applying systemic siRNA approaches, or by placement of synthetic networks in these cells. The latter option is currently explored and will show new promises for smart treatment of vascular disease, like atherosclerosis. A first benchmark study showed promising results as new signalling pathways were identified.

Acknowledgement

References

[1] van Bochove, G.S., Straathof, R., Krams, R., Nicolay, K. and Strijkers, G.J. (2010) Mri-determined carotid artery flow velocities and wall shear stress in a mouse model of vulnerable and stable atherosclerotic plaque. MAGMA 23, 77–84.

[2] Finn, A.V., Nakano, M., Narula, J., Kolodgie, F.D. and Virmani, R. (2010) Concept of vulnerable/unstable plaque. Arterioscler. Thromb. Vasc. Biol. 30, 1282–1292.

[3] Tracqui, P., Broisat, A., Toczek, J., Mesnier, N., Ohayon, J. and Riou, L. (2011) Mapping elasticity moduli of atherosclerotic plaque in situ via atomic force microscopy. J. Struct. Biol. 174, 115–123.

[4] Cuisset, T., Beauloye, C., Melikian, N., Hamilos, M., Sarma, J., Sarno, G., Naslund, M., Smith, L., Van de Vosse, F., Pijls, N.H. and De Bruyne, B. (2009) In vitro and in vivo studies on thermistor-based intracoronary temperature measurements: Effect of pressure and flow. Catheter. Cardiovasc. Interv. 73, 224–230.

[5] Schaar, J.A., Mastik, F., Regar, E., den Uil, C.A., Gijsen, F.J., Wentzel, J.J., Serruys, P.W. and van der Stehen, A.F. (2007) Current diagnostic modalities for vulnerable plaque detection. Curr. Pharm. Des. 13, 995–1001.

[6] Thim, T. (2010) Human-like atherosclerosis in minipigs: A new model for detection and treatment of vulnerable plaques. Dan. Med. Bull. 57, B4161.

[7] Chatzizisis, Y.S. and Giannoglou, G.D. (2010) Shear stress and inflammation: Are we getting closer to the prediction of vulnerable plaque? Expert. Rev. Cardiovasc. Ther. 8, 1351–1353.

[8] Liang, C., Xiaonan, L., Xiaojun, C., Changjiang, L., Xinsheng, X., Guihua, J., Xiaobo, H., Yanen, Z., Runyi, S., Huixia, L., Yun, Z. and Mei, Z. (2009) Effect of metoprolol on vulnerable plaque in rabbits by changing shear stress around plaque and reducing inflammation. Eur. J. Pharmacol. 613, 79–85.

[9] Gao, H., Long, Q., Graves, M., Gillard, J.H. and Li, Z.Y. (2009) Carotid arterial plaque stress analysis using fluid-structure interactive simulation based on in-vivo magnetic resonance images of four patients. J. Biomech. 42, 1416–1423.

[10] Groen, H.C., Gijsen, F.J., van der Lugt, A., Ferguson, M.S., Hatsukami, T.S., van der Steen, A.F., Yuan, C. and Wentzel, J.J. (2007) Plaque rupture in the carotid artery is localized at the high shear stress region: A case report. Stroke 38, 2379–2381.

[11] Segers, D., Helderman, F., Cheng, C., van Damme, L.C., Tempel, D., Boersma, E., Serruys, P.W., de Crom, R., van der Steen, A.F., Holvoet, P. and Krams, R. (2007) Gelatinolytic activity in atherosclerotic plaques is highly localized and is associated with both macrophages and smooth muscle cells in vivo. Circulation 115, 609–616.

[12] Krams, R., Schaar, J., Helderman, F., Cheng, C., Gourabi, B.M., Van Damme, L.C.A., Segers, D., Regar, E., Slager, C.J., de Feyter, P.J., van der Steen, A.F.W. and Serruys, P.W. (2006) Visualization of the vulnerable plaque. Cardiovasc. Res.: New Technol., Methods, and Appl., 221–234.

[13] Cheng, C., Tempel, D., van Haperen, R., van der Baan, A., Grosveld, F., Daemen, M.J.A.P., Krams, R. and de Crom, R. (2006) Atherosclerotic lesion size and vulnerability are determined by patterns of fluid shear stress. Circulation 113, 2744–2753.

[14] Cheng, C., Tempel, D., van Damme, L., van Gaalen, K., van Haperen, R., Krams, R. and de Crom, R. (2005) Angiotensin ii induces severe intra-plaque hemorrhages in lesions with a vulnerable plaque phenotype in apoe ko mice. Circulation 112. U221.

[15] Krams, R., Segers, D., Mousavi Gourabi, B., Maat, W., Cheng, C., van Pelt, C., van Damme, L.C., de Feyter, P., de Feyter, P., van der Steen, T., de Korte, C.L. and Serruys, P.W. (2003) Inflammation and atherosclerosis: Mechanisms underlying vulnerable plaque. J. Interv. Cardiol. 16, 107–113.

[16] Yamazaki, M. and Uchiyama, S. (2010) Pathophysiology of carotid stenosis. Brain Nerve. 62, 1269–1275.

[17] Spence, J.D. (2010) Asymptomatic carotid stenosis: Mainly a medical condition. Vascular 18, 123–126. discussion 127–129..

[18] Montecucco, F., Lenglet, S., Gayet-Ageron, A., Bertolotto, M., Pelli, G., Palombo, D., Pane, B., Spinella, G., Steffens, S., Raffaghello, L., Pistoia, V., Ottonello, L., Pende, A., Dallegri, F. and Mach, F. (2010) Systemic and intraplaque mediators of inflammation are increased in patients symptomatic for ischemic stroke. Stroke 41, 1394–1404.

[19] Sumpio, B.E., Yun, S., Cordova, A.C., Haga, M., Zhang, J., Koh, Y. and Madri, J.A. (2005) Mapks (erk1/2, p38) and akt can be phosphorylated by shear stress independently of platelet endothelial cell adhesion molecule-1 (cd31) in vascular endothelial cells. J. Biol. Chem. 280, 11185–11191.

[20] Shyy, J.Y. and Chien, S. (2002) Role of integrins in endothelial mechanosensing of shear stress. Circ. Res. 91, 769–775.

[21] Gudi, S.R., Clark, C.B. and Frangos, J.A. (1996) Fluid flow rapidly activates g proteins in human endothelial cells. Involvement of g proteins in mechanochemical signal transduction. Circ. Res. 79, 834–839.

[22] Chiu, J.J. and Chien, S. (2011) Effects of disturbed flow on vascular endothelium: Pathophysiological basis and clinical perspectives. Physiol. Rev. 91, 327–387.

[23] Dhawan, S.S., Avati Nanjundappa, R.P., Branch, J.R., Taylor, W.R., Quyyumi, A.A., Jo, H., McDaniel, M.C., Suo, J., Giddens, D. and Samady, H. (2010) Shear stress and plaque development. Expert Rev. Cardiovasc. Ther. 8, 545–556.

[24] Lehoux, S. and Tedgui, A. (2003) Cellular mechanics and gene expression in blood vessels. J. Biomech. 36, 631–643.

[25] Johnson, B.D., Mather, K.J. and Wallace, J.P. (2011) Mechanotransduction of shear in the endothelium: Basic studies and clinical implications. Vasc. Med. 16, 365–377.

[26] Davies, P.F. (2009) Hemodynamic shear stress and the endothelium in cardiovascular pathophysiology. Nat. Clin. Pract. Cardiovasc. Med. 6, 16–26.

[27] Wang, N., Miao, H., Li, Y.S., Zhang, P., Haga, J.H., Hu, Y., Young, A., Yuan, S., Nguyen, P., Wu, C.C. and Chien, S. (2006) Shear stress regulation of kruppel-like factor 2 expression is flow pattern-specific. Biochem. Biophys. Res. Commun. 341, 1244–1251.

[28] Civelek, M., Manduchi, E., Riley, R.J., Stoeckert Jr., C.J. and Davies, P.F. (2011) Coronary artery endothelial transcriptome in vivo: Identification of endoplasmic reticulum stress and enhanced ros by gene connectivity network analysis. Circ Cardiovasc Genet. 4, 243–252.

[29] Wu, F.T., Stefanini, M.O., Mac Gabhann, F., Kontos, C.D., Annex, B.H. and Popel, A.S. (2010) A systems biology perspective on svegfr1 Its biological function, pathogenic role and therapeutic use. J. Cell. Mol. Med. 14, 528–552.

[30] Nikolsky, Y. and Kleemann, R. (2010) Systems biology approaches to the study of cardiovascular drugs. Methods Mol. Biol. 662, 221–243.

[31] Kassab, G.S. (2009) A systems approach to tissue remodeling. J. Biomech. Eng. 131, 101008.

[32] Venet, D., Pecasse, F., Maenhaut, C. and Bersini, H. (2001) Separation of samples into their constituents using gene expression data. Bioinformatics 17, S279–S287. Suppl 1.

[33] Gaujoux, R. and Seoighe, C. (2012) Semi-supervised nonnegative matrix factorization for gene expression deconvolution: A case study. Infect Genet Evol. 12, 913–921.

[34] Zhao, Y. and Simon, R. (2010) Gene expression deconvolution in clinical samples. Genome Med. 2, 93.

[35] Krumsiek, J., Suhre, K., Illig, T., Adamski, J. and Theis, F.J. (2011) Gaussian graphical modeling reconstructs pathway reactions from high-throughput metabolomics data. BMC Syst. Biol. 5, 21.

[36] Zoppoli, P., Morganella, S. and Ceccarelli, M. (2010) Timedelay-aracne: Reverse engineering of gene networks from time-course data by an information theoretic approach. BMC Bioinformatics 11, 154.

[37] Orman, M.A., Berthiaume, F., Androulakis, I.P. and Ierapetritou, M.G. (2011) Advanced stoichiometric analysis of metabolic networks of mammalian systems. Crit. Rev. Biomed. Eng. 39, 511–534.

[38] Tenazinha, N. and Vinga, S. (2011) A survey on methods for modeling and analyzing integrated biological networks. IEEE/ACM Trans. Comput. Biol. Bioinform. 8, 943–958.

[39] Gianchandani, E.P., Chavali, A.K. and Papin, J.A. (2010) The application of flux balance analysis in systems biology. Wiley Interdiscip. Rev. Syst. Biol. Med. 2, 372–382.

[40] Terzer, M., Maynard, N.D., Covert, M.W. and Stelling, J. (2009) Genome-scale metabolic networks. Wiley Interdiscip. Rev. Syst. Biol. Med. 1, 285–297.

[41] Cheng, C., Tempel, D., van Haperen, R., de Boer, H.C., Segers, D., Huisman, M., van Zonneveld, A.J., Leenen, P.J.M., van der Steen, A., Serruys, P.W., de Crom, R. and Krams, R. (2007) Shear stress-induced changes in atherosclerotic plaque composition are modulated by chemokines. J. Clin. Invest. 117, 616–626.

[42] van Bochove, G.S., Straathof, R., Krams, R., Nicolay, K. and Strijkers, G.J. (2010) Mri-determined carotid artery flow velocities and wall shear stress in a mouse model of vulnerable and stable atherosclerotic plaque. Magn. Reson. Mater. Phys., Biol. Med. 23, 77–84.

[43] Hilioti, Z., Sabbagh Jr., W., Paliwal, S., Bergmann, A., Goncalves, M.D., Bardwell, L. and Levchenko, A. (2008) Oscillatory phosphorylation of yeast fus3 map kinase controls periodic gene expression and morphogenesis. Curr. Biol. 18, 1700–1706.

[44] Nelson, D.E., Ihekwaba, A.E., Elliott, M., Johnson, J.R., Gibney, C.A., Foreman, B.E., Nelson, G., See, V., Horton, C.A., Spiller, D.G., Edwards, S.W., McDowell, H.P., Unitt, J.F., Sullivan, E., Grimley, R., Benson, N., Broomhead, D., Kell, D.B. and White, M.R. (2004) Oscillations in nf-kappab signaling control the dynamics of gene expression. Science 306, 704–708.

[45] Bodenstein, C., Knoke, B., Marhl, M., Perc, M. and Schuster, S. (2010) Using jensen's inequality to explain the role of regular calcium oscillations in protein activation. Phys. Biol. 7, 036009.

[46] Parekh, A.B. (2011) Decoding cytosolic ca2+ oscillations. Trends Biochem. Sci. 36, 78–87.

[47] Lewis, R.S. (2003) Calcium oscillations in t-cells: Mechanisms and consequences for gene expression. Biochem. Soc. Trans. 31, 925–929.

[48] Kobayashi, T. and Kageyama, R. (2009) Dynamic advances in nf-kappab signaling analysis. Sci. Signal. 2, pe47.

[49] Abbas, A.R., Wolslegel, K., Seshasayee, D., Modrusan, Z. and Clark, H.F. (2009) Deconvolution of blood microarray data identifies cellular activation patterns in systemic lupus erythematosus. PLoS ONE 4, e6098.

[50] Jain, T., McBride, R., Head, S. and Saez, E. (2009) Highly parallel introduction of nucleic acids into mammalian cells grown in microwell arrays. Lab Chip 9, 3557–3566.

[51] Roy, S., Lane, T., Allen, C., Aragon, A.D. and Werner-Washburne, M. (2006) A hidden-state markov model for cell population deconvolution. J. Comput. Biol. 13, 1749–1774.

[52] Hiller, D., Jiang, H., Xu, W. and Wong, W.H. (2009) Identifiability of isoform deconvolution from junction arrays and rna-seq. Bioinformatics 25, 3056–3059.

[53] Havilio, M. (2006) Signal deconvolution based expression-detection and background adjustment for microarray data. J. Comput. Biol. 13, 63–80.

[54] Wang, H., Hubbell, E., Hu, J.S., Mei, G., Cline, M., Lu, G., Clark, T., Siani-Rose, M.A., Ares, M., Kulp, D.C. and Haussler, D. (2003) Gene structure-based splice variant deconvolution using a microarray platform. Bioinformatics 19, i315–i322. Suppl 1.

[55] Erkkila, T., Lehmusvaara, S., Ruusuvuori, P., Visakorpi, T., Shmulevich, I. and Lahdesmaki, H. (2010) Probabilistic analysis of gene expression measurements from heterogeneous tissues. Bioinformatics 26, 2571–2577.

[56] Shen-Orr, S.S., Tibshirani, R., Khatri, P., Bodian, D.L., Staedtler, F., Perry, N.M., Hastie, T., Sarwal, M.M., Davis, M.M. and Butte, A.J. (2010) Cell type-specific gene expression differences in complex tissues. Nat. Methods 7, 287–289.